Journal of Applied Polymer Science

Plasma-Brominated Cyclo-Olefin Polymer Slides: Suitable Macroinitiators for Activator Regenerated by Electron Transfer/Atom Radical Transfer Polymerization

Christian Heise,[1] Uwe Schedler,[1] Sascha Wettmarshausen,[2] Jörg F. Friedrich[2]
[1]PolyAn GmbH, Rudolf-Baschant-Strasse 2, Berlin 13086, Germany
[2]Federal Institute for Materials Research and Testing, Unter den Eichen 87, 12205, Berlin, Germany
Correspondence to: C. Heise (E-mail: c.heise@poly-an.de)

ABSTRACT: Activators regenerated by electron transfer–atom radical transfer polymerization (ATRP) as a controlled living polymerization are distinguished by their acceptance of small amounts of transition-metal complexes and oxygen and by their tolerance of reducing agents at a high concentration. The precondition of all ATRP applications is the use of homolytic or heterolytic cleavable halides as a dormant species; this allows the propagation of monomer chains. Hence, alkyl bromides are slightly cleavable and are the preferred initiators for ATRP. The bromination of polymer slides used as macroinitiators was carried out under gentle bromoform plasma conditions. This led to an oxidation-resistant stable bromine layer. More than 20 bromines per 100 carbons on the polymer scaffold were permanently bound to the substrate after plasma treatment. The resulting amounts of secondary and tertiary bromines on the polymer scaffold exhibited a suitable macroinitiator concentration for the surface-initiated polymerization of methyl methacrylate and glycidyl methacrylate. © 2014 Wiley Periodicals, Inc. J. Appl. Polym. Sci. **2014**, *131*, 40662.

KEYWORDS: copolymers; functionalization of polymers; grafting; monolayers and polymer brushes; radical polymerization

Received 17 October 2013; accepted 28 February 2014
DOI: 10.1002/app.40662

INTRODUCTION

Atom transfer radical polymerization (ATRP) as a controlled living radical polymerization is characterized by its well-defined polymers with narrow molecular weight distributions (MWDs) and (co)polymers with precisely controlled architectures, functionalities, topologies, and compositions.[1–6] ATRP is less susceptible to large amounts of monomers and initiators, wide ranges of reaction temperatures, and different solvents and dispersed media.[7] Moreover, ATRP is suited for surface modification, bioconjugation, and the preparation of new nanostructured materials that are not accessible by conventional free-radical polymerization. Thus, a plethora of new functional materials has been prepared.[8–11] The reaction is based on the establishment of a rapid equilibration between a minute amount of growing radicals and a majority of dormant species, for example, alkyl halides (R—X). Free radicals are generated through a reversible redox process by a transition-metal complex, for example, a Cu(I)—X ligand, which undergoes a one-electron oxidation with the concomitant abstraction of a halogen atom from the dormant species R—X. Typically, complexing ligands are π-accepting, chelating nitrogen-based ligands, aliphatic polyamines, or simple amines, and this leads to higher polymerization rates.[12,13] In reactions, a reduced-state metal complex is added as an activator, which reacts reversibly with R—X to generate a deactivator and an active radical (R&fradic;); this enables the propagation of the polymer chain (Figure 1). Termination reactions also occur, but they can be minimized by faster deactivation to the dormant species R—X. Other side reactions may limit the achievable molecular weights. However, the main drawback of ATRP is its susceptibility to oxygen. In the presence of air, the reactive metal species (reduced state) is trapped by oxidation (Figure 1). Thus, the use of reducing agents will overcome inhibition by oxygen. As recently reported, in the presence of oxygen, reducing agents [e.g., tin(II) ethyl hexanoate, L-ascorbic acid], oxidized metal complexes, and surplus oxygen are reduced in the reaction vessels.[14] This atom-generated radical polymerization (AGET–ATRP) starts after an introduction period, in which the reduced metal species is rapidly oxidized while oxygen consumption begins. However, the latter is quickly reduced back to an activator (Figure 1). However, in an activator regenerated by electron transfer (ARGET)–ATRP, only a small amount of the activator is permanently regenerated during polymer propagation. A sufficient excess of reducing agents advantageously scavenges oxygen and emerged radicals. In contrast to AGET, ARGET–ATRP tolerates a large excess of reducing agents and might be an appropriate approach

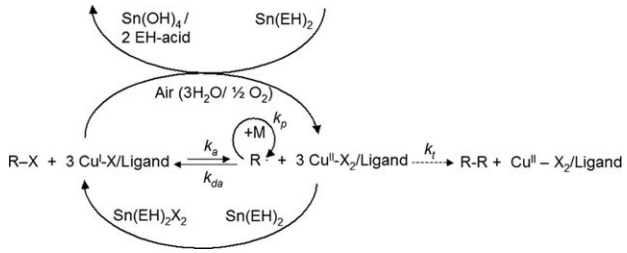

Figure 1. AGET–ATRP reaction (R—X = alkyl halide as dormant species; Cu^{I}—X/ligand = activator that can be oxidized; Cu^{II}—X_2/ligand = deactivator that can be reduced; R • = monomer radical; M = monomer; k_a = activation rate coefficient; k_{da} = deactivation rate coefficient; k_p = polymerization rate coefficient; k_t = termination rate coefficient; EH = ethyl hexanoate).

for surface grafting because the reactor vessels do not need to be deoxygenated.[15]

In this article, we report that plasma bromoform-treated cycloolefin polymer (COP) slides are suitable macroinitiators for surface grafting via ARGET–ATRP. Controlled polymerization in the presence of air is a method for surface grafting and surface modification in an upscaled manner. In general, the polymerization rate of the initiators obeys the first order. To obtain well-defined polymers with narrow MWDs, the halide must rapidly and selectively migrate between the growing chain and the oxidized metal species. Hence, only halides that undergo homolytic or heterolytic cleavage can be used.[16] For molecular weight control, α-carbon substituted and polyhalogenated bromine or chlorine are preferred initiators.[7] Because polymers possess optical properties and a transparency similar to those of glass, polymer supports provide suitable, versatile, cost-saving, and attractive alternatives to commercial glasses. However, the introduction of functional groups (e.g., carboxyls, amines, hydroxyl, halogens) onto the polymer surface occurs under obviously harsh chemistries. In the presence of chromosulfuric acid or other oxidizing acids (e.g., Caro's acid C—C and C—H— bonds), the functional groups are broken and subsequently oxidized to C—O_x.[17] Also, gas-phase oxidations by butane or propane polymer surfaces introduce oxidized chemical species. Furthermore, corona-discharge and energy-rich radiation leads to a broad spectra of surface functionalities.[19–21] Certainly, all of these treatments degrade the polymer surface and, up to 12–67 eV, also the inner scaffold of the polymer. Over time, the introduced functional species turn into polymers to reach the energy lowest state. Hence, after a certain time period, no chemical functionalities are exposed. Additionally, postoxidations of the introduced chemical modifications will be observed. At the least, such modifications are unstable for storage.[22,23] However, surface modifications in plasma or low-pressure plasma processes present a gentle introduction of chemical functionalities. The main advantage of plasma treatments is their selective employment of precursors that enhance the introduction of elected functionalities. The ideal case is the selective substitution of applied precursors. Bromoform ($HCBr_3$), in combination with bromine, as a precursor for bromination, has a low ionization potential of 10.5 eV (1013 kJ/mol). Therefore, a lower electron energy in the plasma is necessary for polyolefin surface modification, and a reduced surface degradation is expected. The bromination of polymer surfaces has other advantages as well. In most compounds, bromine exists in a reduced form and can be oxidized only under extreme conditions. Because of the very low boiling point of bromoform (−76°C), byproducts can be easily removed by an applied vacuum. Bromine, as a neutral precursor, contains a high molar portion of molecular bromine, which is less corrosive than elemental halogen. With the realization of the ideal electronic saturation of the outer shell as the next noble gas configuration, more C—Br bonds are observed. Also, gas radicals in the polymer scaffold can be scavenged by bromine, and this leads to more C—Br groups (Figure 2). Additionally, because of the lower binding energy between C—Br and C—H in $HCBr_3$, a single bromine substitution of polyolefin scaffold is most likely to be $HCBr_3$ + Plasma → $HCBr_2$• + Br• and then $HCBr_3$ + Plasma → CBr_3• + H•. Bromine has an electrophilic character and attacks the polymeric scaffold with a preferred high electron density. Thus, the tertiary C—H bonds are attacked 1600 times faster and secondary C—H bonds are attacked 32 times faster than primary C—H bonds.[24] These secondary and tertiary bromine substitutions are necessary preconditions for applied ATRP in general.[25]

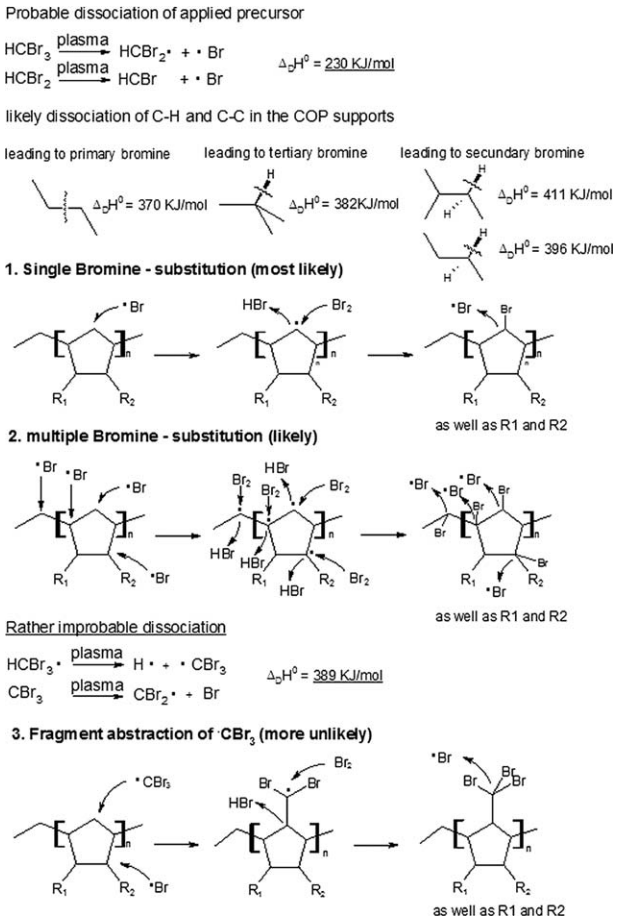

Figure 2. Surface modification of the plasma-induced bromination of the COPs synthesized by the ring-opening metathesis polymerization of various cyclic monomers followed by hydrogenation (R_1 and R_2 are aliphatic residues).[26] ΔH_D^0 = dissociation enthalpy

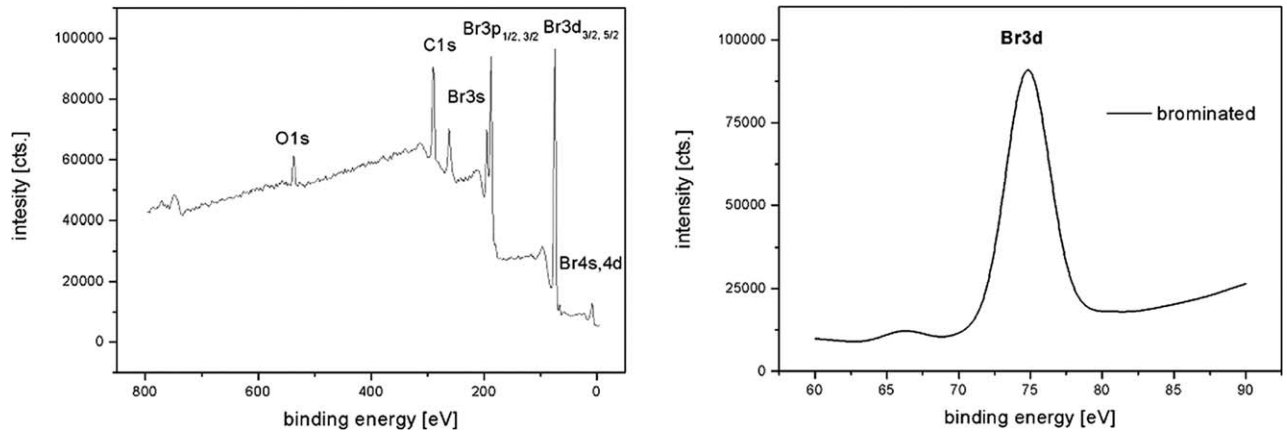

Figure 3. XPS of COP after surface bromination with the bromoform.

Finally, a low-plasma-initiated functionalization is relatively selective because of the thermodynamics of this reaction.[18] The X-ray photoelectron spectroscopy (XPS) analysis in Figure 3 shows that in addition to the C1 peak, two bromine peaks ($Br3p_{1/2}$ and $Br3p_{3/2}$ and $Br3d_{3/2}$ and $Br3d_{5/2}$) are observed; this indicates the existence of C—Br species at the surface. Computer-aided surface analysis for photoelectron spectroscopy (CasaXPS) of the C1 peak presents the distribution and quantification of different carbon species after plasma treatment (Figure 4). These stable bromine species on COP allow a selective and specific three-dimensional (3D) modification with grafted monomers via ATRP. In contrast to glass slides, ARGET–ATRP grafted functional monomers can play an important role in the production of polymer biochips, which require safety regulations in handling.

Under these gentle bromoform plasma conditions, in this study, more than 20% of all introduced bromines could be used for grafting reactions (Figure 5).[27] Because of the radical scavenging by Br atoms. oxidations by the exposure of the polymer to air were hindered.

Other side reactions and the trapping of radicals were only marginally present when bromination was used.[28,29] After plasma treatment, the selective substitution patterns of bromine were used for the ARGET–ATRP propagation of the polymer chain of methyl methacrylate (MMA) or glycidyl methacrylate (GMA); these are demonstrated in the reaction setup in Figure 6.

The High-Throughput microArraying (HTA12) slides were planar COP supports with 12 cavities, which came from Greiner BioOne. The small reaction chambers were used for the analysis of surface grafting and negative controls.

For ARGET–ATRP, plasma-brominated HTA12–COP slides were transferred to slide containers with a total filling volume of 30 mL. After the brominated slides were positioned, the monomer solution was poured, and the transition-metal complex was added to the slide containers, the free headspace resulted in an approximately 25 mL of air. For a more homogeneous chain propagation, we used the halogen-exchange technique. Because the equilibrium constant for chloromacroinitiators was 1–2 orders lower than that of the bromomacroinitiators, C—Cl bonds formed upon the deactivation of the growing chain were reactivated more slowly, and this resulted in a more uniform chain length and polydispersity index (PDI).[30] For that case, we

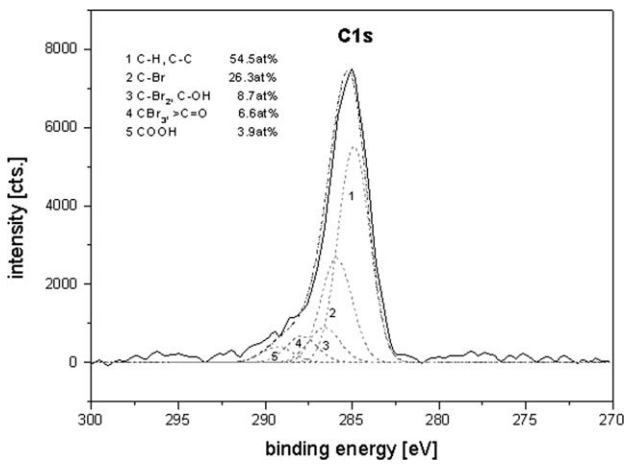

Figure 4. CasaXPS-fitted C1 peak with the peak integration of the COP after surface bromination with the bromoform.

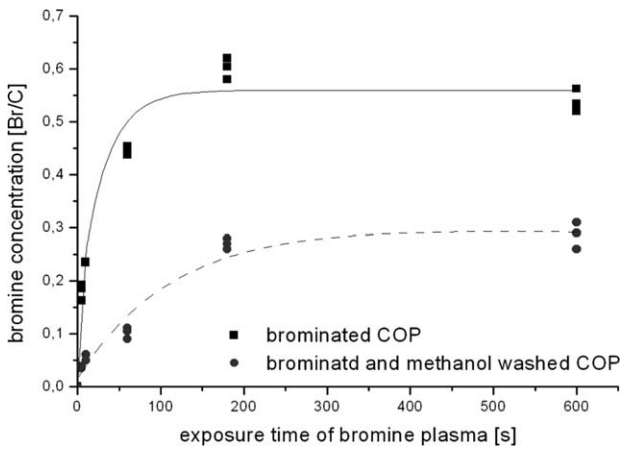

Figure 5. Bromine plasma treatment of COP and washing procedure for the removal of unbound bromine. The remaining concentration of substituted bromine on COP was approximately 20%. After washing, the slides appeared to have a slightly brown shimmer.

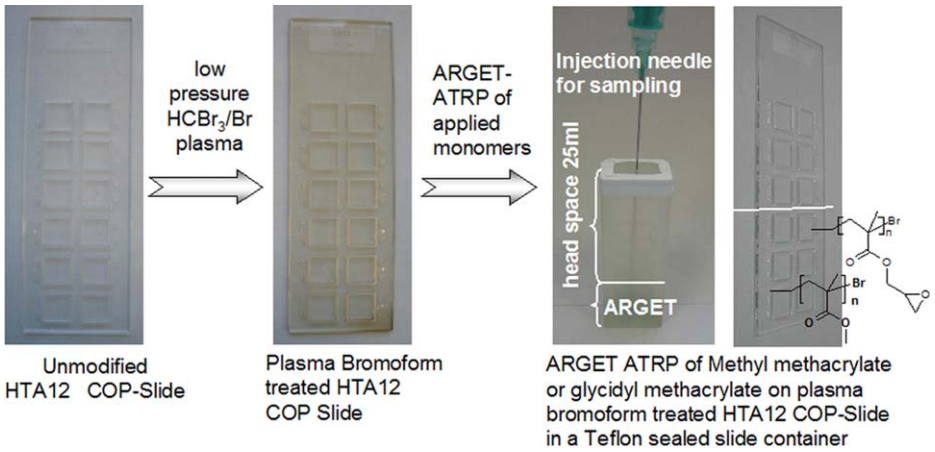

Figure 6. Experimental setup of ARGET–ATRP on the HTA12 COP slides. [Color figure can be viewed in the online issue, which is available at wileyonlinelibrary.com.]

started with a bromine macroinitiator for the proper initiation and replaced the halogen with a chloride during chain propagation for a more controlled surface polymerization[30] (Figure 7).

The ARGET–ATRP was initiated with distinct amounts (100–200 μL or 0.3–0.9 mmol) of tin(II) 2-ethylhexanoate. The grafted polymer layers of MMA and GMA were characterized by gel permeation chromatography (GPC), attenuated total reflectance (ATR)–Fourier transform infrared (FTIR), spectroscopy, Coomassie staining, and reaction with fluorescence dyes.

EXPERIMENTAL

Materials

MMA (>97%) and GMA (>97%, Fluka) were purified by passage through an aluminum oxide filled column. The copper ligand 1,1,4,7,10,10-hexamethyltriethyl tetramine (HMTETA; 97%) was purchased from Aldrich, and copper(II) chloride (>99%, Fluka) and tin(II) 2-ethyl hexanoate were purchased from Sigma (95%) All other chemicals were used as received. COP slides with 12 cavities and slide containers as reaction chambers were provided by Greiner BioOne (Greiner GmbH, Frickenhausen, Germany).

For the surface substitution with bromine, bromoform was used as a precursor. The bromination of the COP slides was conducted in a bell-jar reactor with internal electrodes working at 13.56 MHz. The pressure within the plasma reactor was aligned to 2–20 Pa, the power input was in the range 10–300 W, and the treatment time was between 2 and 500 s. The slide was fixed and allowed to rotate through the plasma zone mounted on a rotating steel cylinder. Under these conditions, the emerged radicals were saturated to C—Br, and postoxidations efficiently reduced during the formation of HBr were purged off by the applied low pressure. The surface-initiated ARGET–ATRP of MMA and GMA were conducted in slide containers; each of them contained a filling volume of 30 mL. Primarily, the slide containers were fitted with an injection needle for sampling and to monitor the reaction. After the plasma-brominated slides were positioned, the containers were filled with 4.1 mL (38 mmol) of methyl methacrylate for MMA–ARGET–ATRP and 5.0 mL (39 mmol) of GMA for GMA–ARGET–ATRP. A volume of 28 μL (0.19 mmol) of ethyl α-bromoisobutyrate (EBiB) was used as a soluble ATRP initiator for sampling and analytics. Then, a 25.5 mg/mL stock solution of $Cu(II)Cl_2$ (0.19 mmol) in an Aceton Plus and 52 μL of HMTETA (0.19 mmol) were freshly prepared. Distinct molar amounts of the prepared copper complex were added to the monomer solution in the containers; the reaction was initiated with tin(II) 2-ethylhexanoate, the container was subsequently sealed with a Teflon tape, and the mixture was reacted at room temperature for several hours. Samples were taken with the injection needle after 22, 25, and 40 h of reaction time for MMA–ARGET–ATRP (Table I, entries

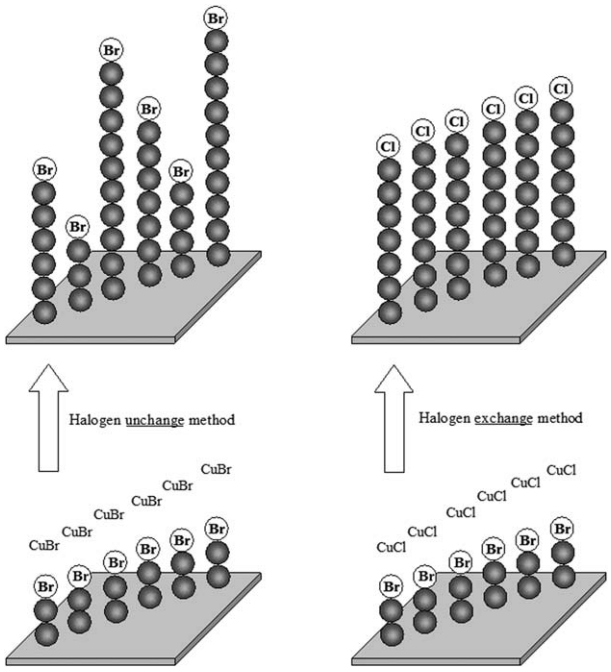

Figure 7. Principle of ARGET–ATRP with the halogen exchange method for a lower PDI and better control of the chain length. The equilibrium constant for the alkyl chloride initiators was 1–2 orders lower than that of the alkyl bromide initiators. Thus, the C—Cl formed upon deactivation reacted more slowly and led, therefore, to a more defined chain length with a narrow MWD and a lower polydispersity.[30]

Table I. ARGET–ATRP Properties of MMA and GMA at Room Temperature

Entry	MMA	EBiB	$CuCl_2$	$[Sn(EH)2]_0/[EBiB]_0$ molar ratio	$CuCl_2$ (ppm)	Time (h)	Conversion (%)	M_n	M_w	PDI (M_w/M_n)
1	200	1	0.01	3.3	50	25	19	41,660	71,070	1.7
2	200	1	0.01	3.3	50	40	34	50,130	70,780	1.41
3	200	1	0.02	4.9	100	22	52	33,910	50,060	1.46
Entry	GMA	EBiB	$CuCl_2$	$[Sn(EH)2]_0/[EBiB]_0$ molar ratio	$CuCl_2$ (ppm)	Time (h)	Conversion (%)	M_n	M_w	PDI (M_w/M_n)
4	200	1	0.01	3.3	50	16	87	60,660	186,100	3.06
5	200	1	0.01	4.9	50	8	76	14,680	54,000	3.67

M_w, weight-average molecular weight; M_n, number-average molecular weight; EBiB = ethyl a-bromoisobutyrate.

1–3) and after 8 and 16 h for GMA–ARGET–ATRP (Table I, entries 4 and 5). All of the used brominated COP slides sustained all of the applied chemicals and monomers without any etchings, adsorptions, dissolution, or diffusions into the slides. This was verified in the adsorption tests of GMA and MMA on COP slides over 48 h. In the ATR–FTIR spectra, only bending and valence vibrations of the COP were visible. Hence, no applied methacrylate was adsorbed or diffused into the COP material (valence vibration (ν) = 2865 cm^{-1} for C—H— valence of the CH_3 groups, ν = 2930 cm^{-1} for C—H valence of the CH_2 groups, δ = 1450 cm^{-1} for bendings of the CH_2 groups, and δ = 1350 cm^{-1} for bendings of CH_3; see Figure 8).

The HTA12 slide format was divided into 12 cavities or reactions chambers, which could be separately used for different analysis (shown later in Figures 16 and 17). Because of the risk of crosslinking within the ARGET solution, the formation of byproducts, the participation of side reactions, and the reduction of the oxirane rings, the ARGET–ATRP conditions had to be primarily optimized.[31,32] Therefore, nine 24-mL glass vials with screw caps (ND24 with white PP screw caps from Fisher Scientific) were filled with 5.0 mL (38 mmol) of glycidyl methacrylate and 28 μL (0.19 mmol) of EBiB as a soluble ATRP initiator for sampling and analytics (Figure 9). Defined amounts (50–200 ppm, Table I) of the 25.5 mg/mL stock solution of $Cu(II)Cl_2$ (0.19 mmol) in Aceton Plus and 52 μL of HMTETA (0.19 mmol) were pipetted into glass vials, the reaction was initiated with distinct amounts of tin(II) 2-ethylhexanoate (100–200 μL or 0.3–0.9 mmol), and the vials were sealed with screw caps.

After optimization the GMA–ARGET–ATRP, the derived conditions were transferred to slide surfaces in slide containers, as mentioned previously (Table I, entries 4 and 5). Consequently, the backside of the grafted slides was characterized by ATR–FTIR spectroscopy (PerkinElmer Spectrum One, inclusive universal ATR sampling accessory), atomic force microscopy (AFM) in the tapping mode (Biolyzer SNOM AFM instrument, Triple-O, Potsdam, Germany), and contact angle measurements with water droplets (Contact Angle Systems OCA 20, Data Physics Instruments GmbH, Filderstadt, Germany) while the cavity surface was used for staining. Contact angles of 3 μL water droplets between the surface and tangent of the three border lines (solid–fluid–air) were determined by internal software (Data Physics V.2.1.9 Build 21). Because fluorescence was used as a sensitive indicator for the surface reactions, the temporary gradient of chain propagation was characterized with the reaction of an Alexa 647 Fluor fibrinogen conjugate. Fibrinogen is a glycoprotein with four subunits, and it plays an important role in blood clotting. Moreover, it is a decisive cofactor at the

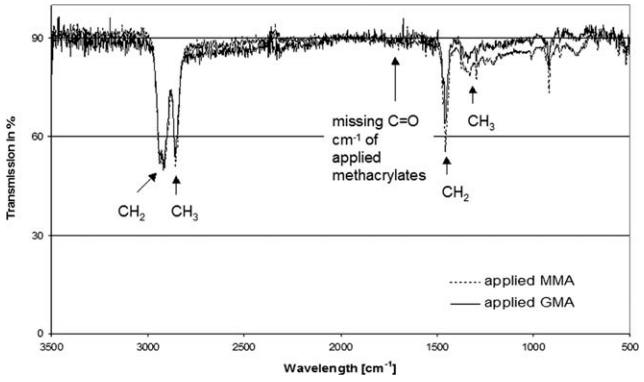

Figure 8. ATR–FTIR spectra of the GMA- and MMA-adsorbed COP slides after 48 h.

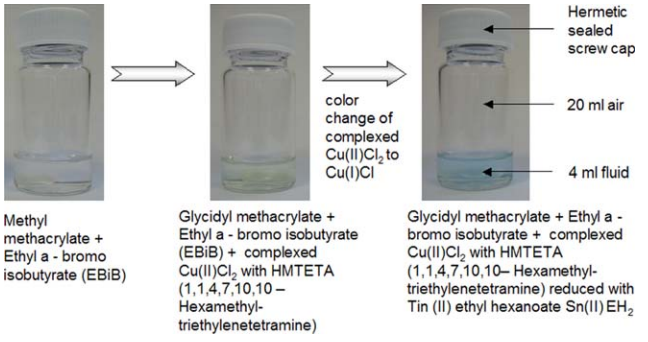

Figure 9. Reaction setup for the GMA–ARGET–ATRP optimization. [Color figure can be viewed in the online issue, which is available at wileyonlinelibrary.com.]

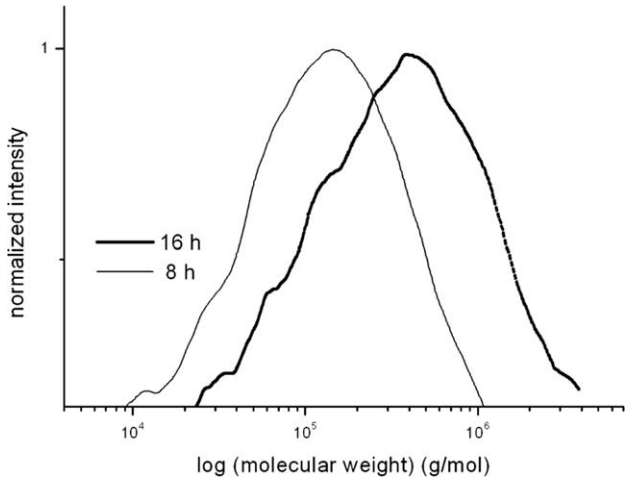

Figure 10. GPC traces of pGMA via ARGET–ATRP.

aggregation of thrombocytes. For the reaction-time-dependent immobilization of this fluorescence dye, the optimized GMA–ARGET–ATRP of entry 4 was processed in five different containers. After certain time periods, the containers were opened. GMA-grafted COP slides were used for the immobilization of the Alexa 647 Fluor fibrinogen conjugate. Hereby, only the cavities A2, B2, A5, and B5 as negative controls were applied with 40 μL of 150 μg/mL Alexa 647 Fluor fibrinogen conjugate. After 2 h of immobilization, the slides were thoroughly rinsed with water, ethanol, and water again and scanned with an Axon slide scanner (Axon Instruments Gene Pix Personal 4100 A, Molecular Devices, Sunnyvale, CA) at an excitation/emission wavelength of 635/670 nm. The pixel intensities were integrated over an area of 30 mm^2 and averaged over the cavities. The grafted cavities A1 and B1 and the nongrafted cavities A6 and B6 were reacted with 1,4-diaminobutane, stained with EZ Blue Coomassie staining reagent, and gently shaken for 2 h in a slide container in a nonfluorescent independent method. Afterward, the slides were washed three times with deionized water.

RESULTS AND DISCUSSION

Typically, the PDI of ARGET–ATRP reactions is near 1. The PDI becomes smaller with increasing monomer conversion and increasing deactivator concentration:

$$\mathrm{PDI} = \frac{M_w}{M_n} = 1 + \left(\frac{[RX]_0 k_0}{k_{\mathrm{deact}}[Mt^{n+1}X/L]}\right)\left(\frac{2}{\mathrm{Conversion}} - 1\right)$$

k_{deact} = constant of deactivation, $[RX]_0$ = hologenated initiator k_0 = constant of propagation Mt^{n+1} = metal in oxidized state, X = halogen and L = ligand. Obviously, the reaction rate of the surface-initiated ARGET–ATRP decreased at room temperature. Because of the possible softening or thermal degradations of the brominated support material, higher temperatures were avoided. The resulting lower conversions are indicated in Table I.

In contrast to the GPC analysis of poly methyl methacrylate (pMMA) (Figure 11), the GPC traces of poly glycidyl methacrylate (pGMA) shown in Figure 10 showed a broader and multimodal MWD, which also resulted in a higher PDI. Tsarevsky and coworkers[33,34] have recently reported that tin (II) 2- ethylhexanoate ($Sn(EH)_2$), as a Lewis acid with a nucleophilic carboxylate counter ion, takes part in the polymerization of GMA and may open the oxirane rings (Figure 1). In a further reaction, the opened ring and the moisture in the headspace can react with intact epoxides; this leads to branched pGMA or crosslinked polymer. With that background, we varied the ratios of $Cu(II)Cl_2$ to $Sn(EH)_2$ to determine the optimized parameters of the uncrosslinked polymers. Obviously, the results in Figure 12 show that higher amounts of complexed $CuCl_2$ led to more crosslinked polymers in the beginning of the polymerization, and higher amounts of $Sn(EH)_2$ resulted in the proceeded chain propagation. Generally, in ATRP, the reduced Cu(I) species undergoes a one-electron oxidation with abstraction of a halogen and a generated radical on the initiator side. However, in the early reaction, the applied oxidized form of $Cu(II)Cl_2$, as a stronger Lewis acid than Cu(I), can also attack the electrophilic bromine in the initiator group, and this leads to partial positivated carbon or a temporary carbenium ion, which can react with nucleophils in solution [e.g., the nucleophilic carboxylate counter ion of $Sn(EH)_2$ or amines of the ligand]. Therefore, higher amounts and an excess of complexing agents for copper (nucleophilic amines and amides) should be avoided. In this case, the remaining bromine may attack the carbon in the oxirane ring in a nucleophilic reaction that is mediated by the occurring ethyl hexanoate (EH) acid and the electrophilic Lewis acids $Cu(II)Cl_2$ and $Sn(EH)_2$, as shown in Figure 1. Investigations with $Sn(EH)_2$ without any Cu–ligand and complexes have shown that $Sn(EH)_2$ is able to open the oxirane rings. If these possible side reactions are decisive and predominant, ATRP is hindered, and no surface grafting occurs. Finally, the moisture in the headspace may hydrolyze the oxiranes diols and force the crosslinking reaction. Crosslinked pGMA cannot be resolved with acetone or tetrahydrofuran, and no polymerized GMA can participate in methanol or ethyl acetate. It should be mentioned that the surface grafting of reactive functional monomers is slightly difficult in the presence of redox systems, and chemical functions must, therefore, be consequently protected. Hence, only a small parameter window is suitable for a controlled GMA surface grafting via ARGET–ATRP.

Figure 9 shows the reaction setup and reaction vessels for ARGET–ATRP in the presence of 20 mL of air (standard

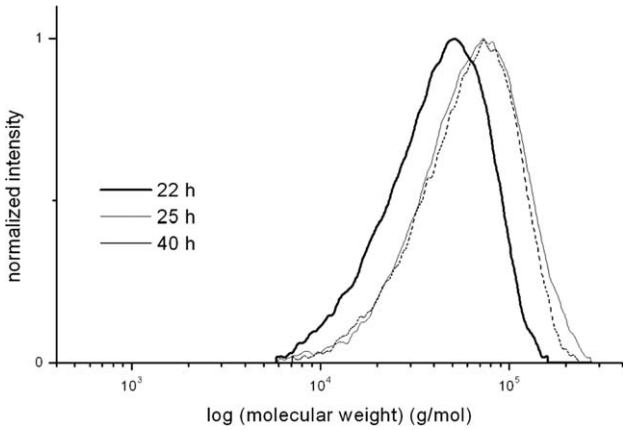

Figure 11. GPC traces of pMMA via ARGET–ATRP.

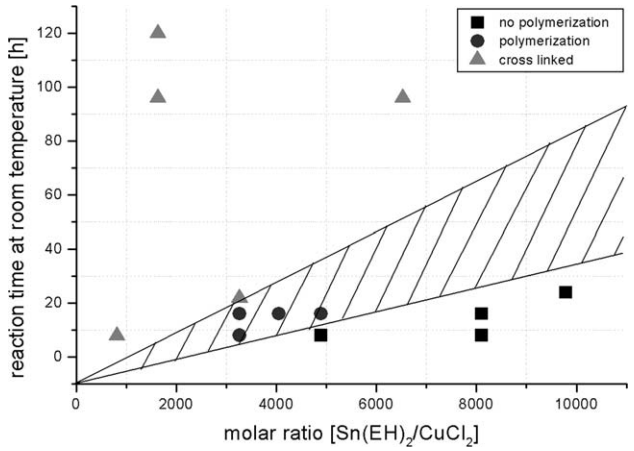

Figure 12. Optimization of GMA–ARGET–ATRP for the surface initiated (SI)–ARGET–ATRP parameter window for the GMA grafting via ARGET–ATRP.

pressure at 101,325 Pa and room temperature = 24°C). The amount of $Sn(EH)_2$ needed to consume oxygen in the headspace and the reduction of the deactivator complied with Boyle's law. With the assumption that the 20 mL of free headspace contained 21% oxygen and that two molecules of $Sn(EH)_2$ reduced one molecule of O_2, 0.34 mmol for 20 mL of air and 0.43 mmol for 25 mL of air of the reducing agent were needed. Additionally, to marginally reduce Cu(II), 3.8 nmol was needed.

The AFM images in Figure 14 show the ARGET–ATRP surface grafting on two slides. The first one was an ARGET–ATRP surface-grafted pMMA on COP without bromination, and the second one was a surface-grafted ARGET–ATRP after bromoform plasma treatment. Obviously, ARGET–ATRP surface grafting did not occur without a sacrificial initiator. The surface roughness of this slide was determined to be 10 nm. The bromoform-treated COP slide presented a 10-fold higher roughness of about 100–150 nm after a grafting time of 40 h. Because the slide dipping depth was determined to be 7.5 cm^2, an area of 20% (1.5 cm^2) was brominated, and this depicted a sacrificial initiator concentration for ARGET–ATRP. Brushes on the COP surfaces were estimated to be 50–100 nm.

Figure 13a,b shows the FTIR spectra of the ARGET–ATRP grafted and nongrafted zones. In contrast to the nonmodified area (the blank), the esters of GMA and MMA (ATR: valence C—O

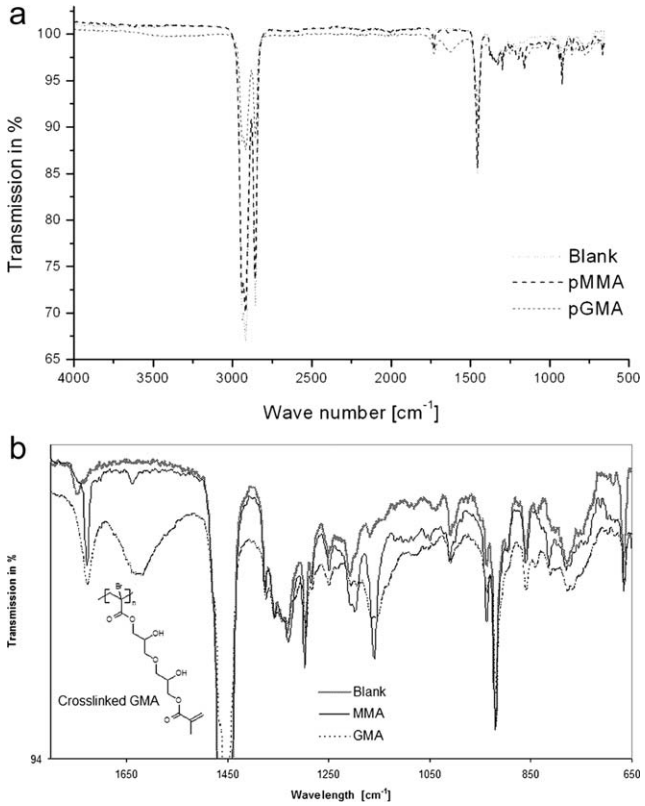

Figure 13. ATR–FTIR spectra of the modified surface area. The negative control (blank) was taken from the nonmodified section.

$\nu = 1729\ cm^{-1}$, valence C—O—C $\nu = 1170\ cm^{-1}$, and asymmetric vibrations epoxy ring $\nu_{epoxi} = 1231\ cm^{-1}$ and $\nu_{epoxi} = 839\ cm^{-1}$). The visible valence vibrations at $\nu = 1637\ cm^{-1}$ indicated that the C=C acrylate bond resulted from of a partly crosslinking reaction of pGMA.[33,34] This aligned with the findings of the GPC of pGMA shown in Figure 10. In the case of pMMA, the C=C band was missing, and this indicated a full polymerization. However, not every epoxy group was crosslinked; this is shown in the following analysis. Contact angle measurements on the backside indicated changed physical behavior between the grafted and nongrafted zones. Although the contact angle in the nongrafted zone remained at 70–75°, the angle changed exactly on the dipping edge to 40–45° in the GMA grafted zone (Figure 15).

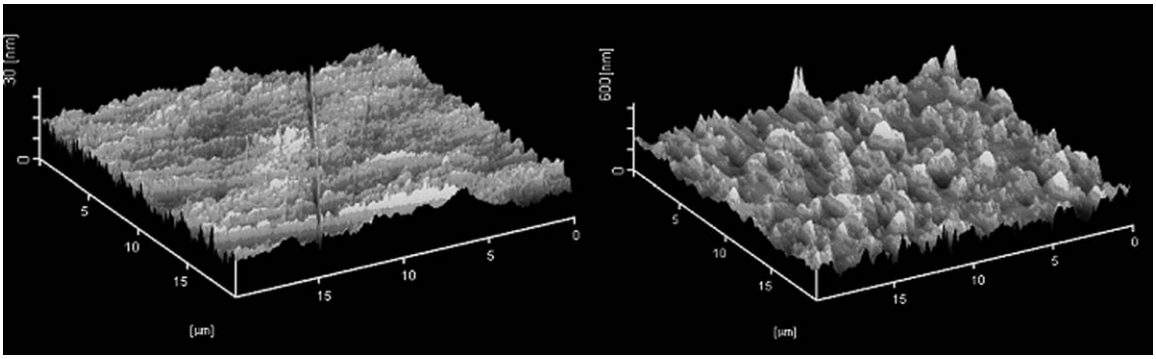

Figure 14. AFM image of the grafted surfaces measured in the tapping mode. The left AFM image presents the surface grafting of MMA on the nonbrominated COP; the right AFM image show the surface grafting of MMA on the brominated COP with the sacrificial initiator concentration.

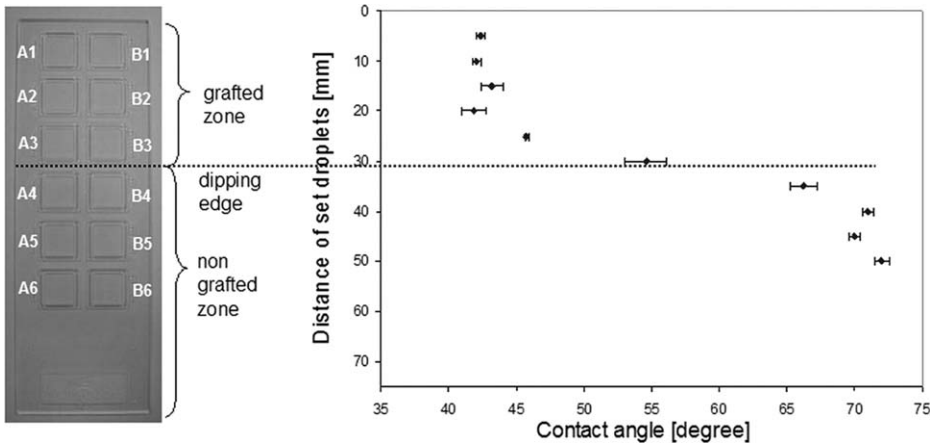

Figure 15. Gradient of the contact angles determined from the backside of a partially grafted slide after 16 h of surface-initiated ARGET–ATRP with GMA.

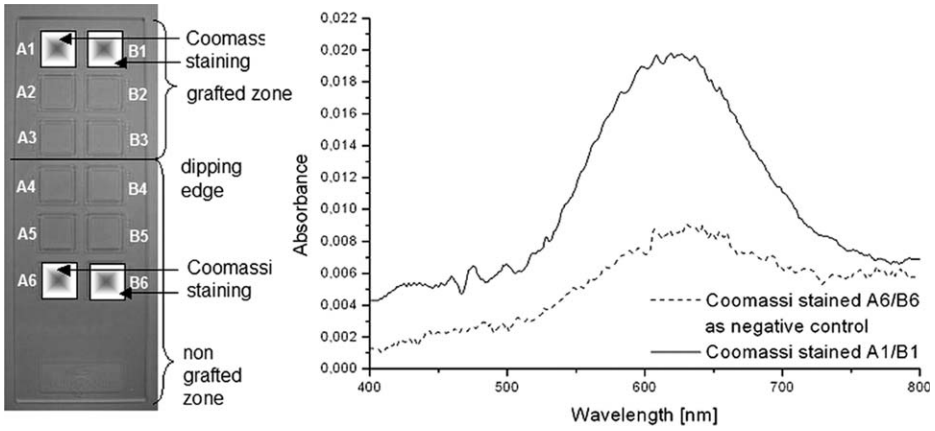

Figure 16. Ultraviolet–visible spectra of the Coomassie-stained cavities. A1/B1 after 16 h of surface-initiated ARGET–ATRP with GMA.

The GMA-grafted section with cavities A1/B1 and the nongrafted area with cavities A6/B6 as the negative control were used for Coomassie staining after the reaction with 1,4-diaminobutane as a second a nonfluorescent and independent analysis of the GMA. Coomassie is a triphenylmethane dye that is commonly used for protein staining. The staining reaction is based on the ionic iteration between the ionic Coomassie dye and the basic amines. Thus, Coomassie staining is a suitable method for

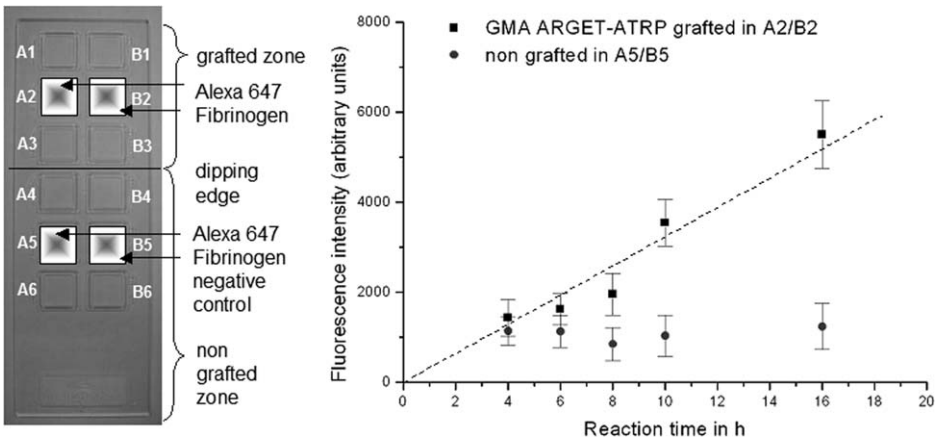

Figure 17. Integrated fluorescence intensity of a coupled Alexa 647 Fluor fibrinogen conjugate in 30 sqmm of A2, B2, A5, and B5 after 16 h of surface-initiated ARGET–ATRP with GMA.

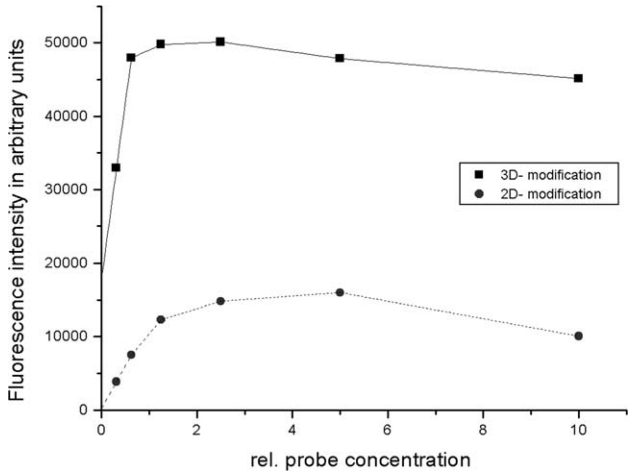

Figure 18. Hybridization efficiency of the immobilized capture probes on the 3D and 2D epoxy surfaces.

UV analysis after interaction with reacted amines on epoxy surfaces. The wavelength scan from 400 to 800 nm presented a typical extinction in the grafted zone at 610 nm during the negative control leave-out (Figure 16).

In selective time periods of ARGET–ATRP, the containers were opened, and the A2, B2, A5, and B5 cavities of every three grafted slides were used for coupling with the Alexa 647 Fluor fibrinogen conjugate. Nongrafted cavities represented by A5 and B5 were used as negative controls. The time-dependent coupling efficiency was shown by the fluorescence intensity of the Alexa 647 Fluor fibrinogen conjugate (arbitrary units). The linear increase of the coupling efficiency indicated a surface grafting via ATRP because the controlled living polymerization obeyed a first-order reaction (Figure 17), whereas the fluorescence signals at 670 nm in the ARGET–ATRP A2 and B2 cavities increased within the reaction time, and the negative controls in A5 and B5 showed no immobilization.

CONCLUSIONS

Because polymer supports have to be functionalized under harsh chemical conditions, ARGET–ATRP of the brominated COP presented a very attractive approach for a mild introduction of chemical functionalities. Under conventional plasma conditions, functional groups may oxidize, degrade the polymer scaffold, or be unstable over long periods. The low-pressure bromoform plasma treatment of COP as a gentle and low-energy method for the introduction of a stable and covalent-bond bromine exhibited suitable macroinitiators for ATRP applications. Furthermore, the functional species of the grafted layer were stable and did not turn into the polymer as in cases of plasma treatments.[35] Additionally, the grafted 3D surface layers were more reactive and exhibited higher coupling efficiencies and homogeneities than the two-dimensional (2D) surface modifications. Figure 18 presents the hybridization efficiencies of dye-labeled oligomers onto immobilized capture probes on 3D epoxy and 2D epoxy layers. The immobilization efficiency and/or hybridization efficiency were much higher over a broad range of probe concentrations, and even lower probe concentrations could be used

Despite the easy handling and mild reaction conditions of ARGET–ATRP, which tolerated oxygen, traces of water, and small amounts of metal complex, the polymerization of GMA or monomers that could be oxidized or deduced were not suited for obtaining distinct molecular chain lengths. The qualitative and quantitative analyses showed that GMA was successfully grafted on COP and applied for the coupling reactions of biochemical species. In particular, the use of a slide container with a moderate presence of oxygen allowed the scale-up of several hundred slides for surface functionalization via ARGET–ATRP in one modification run. Moreover, a homogeneous distribution of functional groups and the adjustment of the functionality density by ARGET–ATRP are useful information and may prove suitability for biochip applications.

ACKNOWLEDGMENTS

The authors thank Greiner BioOne for providing the HTA12 slides.

REFERENCES

1. Matyjaszewski, K.; Davis, T. P. Handbook of Radical Polymerization; Wiley-Interscience: New York, **2002**.
2. Goto, A.; Fukuda, T. *Prog. Polym. Sci.* **2004**, *29*, 329.
3. Wang, J.-S.; Matyjaszewski, K. *J. Am. Chem. Soc.* **1995**, *117*, 5614.
4. Patten, T. E.; Xia, J.; Abernathy, T.; Matyjaszewski, K. *Science* **1996**, *272*, 866.
5. Patten, T. E.; Matyjaszewski, K. *Adv. Mater.* **1998**, *10*, 901.
6. Cossens, V.; Pinthauer, T.; Matyjaszewski, K. *Prog. Polym. Sci.* **2001**, *26*, 337.
7. Matyjaszweski, K.; Xia, J. *J. Chem. Rev.* **2001**, *101*, 2921.
8. Wertheimer, M. R.; Fozza, A. C.; Holländer, A. *Nucl. Instrum. Methods Phys. Res. Sect. B* **1999**, *151*, 65.
9. Matyjaszewski, K. *Prog. Polym. Sci.* **2005**, *30*, 858.
10. Tang, C.; Qi, K.; Wooley, K. L.; Matyjaszewski, K.; Kowalewski, T. *Angew. Chem.* **2004**, *116*, 2843.
11. Pyun, J.; Kowalewski, T.; Matyjaszewski, K. *Macromol. Rapid Commun.* **2003**, *24*, 1043.
12. Nuss, S.; Bottcher, H.; Wurm, H.; Hallensleben, M. L. *Angew. Chem.* **2001**, *113*, 4137.
13. Karlin, K. D.; Zubieta, J. Copper Coordination Chemistry: Biochemical and Inorganic Perspective; Academic: New York, **1983**.
14. Bernhardt, P. V. *J. Am. Chem. Soc.* **1997**, *11*, 771.
15. Min, K.; Jakubowski, W.; Matyjaszewski, K. *Macromol. Rapid Commun.* **2006**, *27*, 594.
16. Matyjaszewski, K.; Dong, H.; Jakubowski, W.; Pietrasik, J.; Kusumo, A. *Langmuir* **2007**, *23*, 4528.
17. Matyjaszewski, K.; Coca, S.; Gaynor, S. G.; Nakagawa, Y.; Jo, S. M. W.O. Pat. 9801480, 1998; U.S. Pat. 5,789,487, **1998**.

18. Fonseca, C.; Perena, F.; Fatou, F. G. *J. Mater. Sci.* **1985**, *20*, 3283.
19. Perena, J. M.; Lorenzo, V.; Zamfirova, G. *Polym. Test* **2000**, *19*, 231.
20. Desai, S. M.; Singh, R. P. *Adv. Polym. Sci.* **2004**, *169*, 231.
21. Kogelschatz, U. *Pure Appl. Chem.* **1990**, *6*, 1667.
22. Chanunpanich, N.; Ulman, A.; Strzhemechny, Y. M. *Langmuir* **1999**, *15*, 1080.
23. Jonsson, M.; Nystroem, V.; Nordin, O.; Malmstroem, E. *Eur. Polym. J.* **2009**, *45*, 2374.
24. Gaudioso, J.; Craighead, H. G. *J. Chromatogr.* **2002**, *971*, 249.
25. Briggs, D. In Practical Surface Analysis; Briggs, D., Seah, M. P., Eds.; Wiley: Chichester, United Kingdom, **1996**; p 437.
26. Tang, W.; Matyjaszewski, K. *Am. Chem. Soc. Div. Polym. Chem* **2005**, *46*, 211.
27. Shin, J. Y.; Park, J. Y.; Liu, C. Y.; He, J. S.; Kim, S. C. *Pure Appl. Chem.* **2005**, *77*, 801.
28. Wettmarshausen, S.; Kühn, G.; Hidde, G.; Mittmann, H.-U.; Friedrich, J. F. *Plasma Process. Polym.* **2007**, *4*, 832.
29. Friedrich, J.; Kühn, G.; Schulz, U.; Jansen, K.; Möller, B. *Vakuum* **2002**, *14*, 285.
30. Braunecker, W. A.; Matyjaszeeski, K. *Prog. Polym. Sci.* **2007**, *32*, 93.
31. Matyjaszewski, K.; Shipp, D. A.; Wang, J.-L.; Grimaud, T.; Patten, T. E. *Macromolecules* **1998**, *31*, 6836.
32. Johansson, B. L.; Larsson, A.; Ocklind, A.; Ohrlund, A. *J. Appl. Polym. Sci.* **2002**, *86*, 2618.
33. Tang, W.; Kwak, Y.; Braunecker, W.; Tsarevsky, N. V.; Coote, M. L.; Matyjaszewski, K. *J. Am. Chem. Soc.* **2008**, *130*, 10702.
34. Tsarevsky, N. V.; Jakubowski, W. *J. Polym. Sci. Part A: Polym. Chem.* **2010**, *49*, 918.
35. Jokinen, V.; Suvanto, P.; Franssila, S. *Biomicrofluidics* **2012**, *6*, 06150101.